frontiers | Frontiers in Marine Science

TYPE Original Research
PUBLISHED 25 April 2023
DOI 10.3389/fmars.2023.1073054

OPEN ACCESS

EDITED BY
Zhiyu Liu,
Xiamen University, China

REVIEWED BY
Xing Jian,
Xiamen University, China
Jingrui Li,
Qingdao National Laboratory for Marine Science and Technology, China
Zhongbo Wang,
Shantou University, China

*CORRESPONDENCE
Zhengxin Yin
yinzhengxin777@163.com

SPECIALTY SECTION
This article was submitted to Physical Oceanography, a section of the journal Frontiers in Marine Science

RECEIVED 18 October 2022
ACCEPTED 28 March 2023
PUBLISHED 25 April 2023

CITATION
Cai Z, Huang Q, Yin Z, Huang X, Chen L and Tang M (2023) The sources and transport pathways of sediment in the northern Ninety-east Ridge of the India Ocean over the last 35000 years. *Front. Mar. Sci.* 10:1073054. doi: 10.3389/fmars.2023.1073054

The sources and transport pathways of sediment in the northern Ninety-east Ridge of the India Ocean over the last 35000 years

Zhourong Cai[1,2,3], Qianru Huang[1,2,3], Zhengxin Yin[4,5]*, Xiaofeng Huang[1,2,3], Liang Chen[4,5] and Meng Tang[4,5]

[1]School of Marine Sciences, Sun Yat-sen University, Zhuhai, China, [2]Southern Laboratory of Ocean Science and Engineering (Zhuhai), Zhuhai, China, [3]Guangdong Provincial Key Laboratory of Marine Resources and Coastal Engineering, Zhuhai, China, [4]South China Sea Marine Survey and Technology Center, State Oceanic Administration, Guangzhou, China, [5]Key Laboratory of Marine Environmental Survey Technology and Application, Ministry of Natural Resources, Guangzhou, China

The Ninety-east Ridge (NER) is located in the southern Bay of Bengal in the northeast Indian Ocean and is composed of pelagic and hemipelagic sediments. In addition to contributions from marine biomass, the ridge also contains terrestrially sourced sedimentary material. However, considerable disagreement remains regarding the origin of these terrestrial materials and transport pathways. This paper discusses the collection of seafloor surface sediments and three sediment cores recovered from the northern region of the NER, as well as the analysis of clay minerals, Sr-Nd isotopes, and sediment grain size. The ages of the three core sediments are constrained by AMS ^{14}C dating to better establish the source and transport pathways of the terrestrial materials within NER sediments over the past 35000 years. The research results show that the Qinghai-Tibet Plateau is the predominate source of terrigenous sedimentary material in the NER. In the plateau, the crustal materials were weathered and stripped and then transported to the Andaman Sea *via* the Irrawaddy River. From there, the material was transported westward by monsoon-driven circulation to the northernmost part of the NER before being transported to the south for final deposition. This transport mode has changed little over the past 35000 years. However, during the rapidly changing climate of the Younger Dryas (12.9~11.5 ka BP), there were some variations in the input amount, grain size, and Sr-Nd isotope value of the source material. The above conclusions are significant for re-evaluating the source of terrigenous sediments, the temporal and spatial changes in transport modes, and the sensitivity of the NER to climatic shifts.

KEYWORDS

Ninety-east Ridge, Bay of Bengal, provenance analysis, transport mode, northeast Indian Ocean, Sr-Nd isotope

1 Introduction

The collision between the Indian and Eurasian plates and the resulting uplift of the Qinghai-Tibet Plateau are among the most important geological events affecting the global climate and environmental change since the Cenozoic era began (Hall, 2002; Clark et al., 2005). The uplift process produced a large volume of sediment *via* weathering and denudation of the landscape. The transportation and deposition of the resultant terrigenous materials into the ocean. This is considered a result of these "source-sink" interactions. The NER in the northeast Indian Ocean is located in the south of the Bay of Bengal. Its pelagic sediments contain records of past rapid palaeoceanographic and palaeoclimatological changes and constitute the sedimentary response of the source-sink process initiated by the uplift of the Qinghai-Tibet Plateau. The NER has important significance in the fields of environmental science, climatology, and geology.

The Bay of Bengal is a semi-enclosed ocean basin bounded at three sides by land and is open at the south, where it is connected to the Indian Ocean. Previous studies have suggested that the seasonally reversing monsoon currents (southwest in June–September and northeast in December–February) plays an important role in sediment and water exchange in the Bay of Bengal and the northern Indian Ocean (Schott and McCreary, 2001; Shankar et al., 2002; Durand et al., 2009; Scott and Xu, 2009; Webber et al., 2018), and the change of the current is also studied by numerical simulation (Prakash and Pant, 2019; Agarwal et al., 2022). In addition, the Bay of Bengal is well-fed with a large volume of freshwater flux from several rivers. Therefore, Large amount of sediment can be transported to the southern Bay of Bengal through currents, tidal and wind waves, and formed the largest sedimentary fan in the world (Curray et al., 2002; Weber et al., 2003).

The sediments of the NER, to the south of the Bengal fan, are mainly pelagic and hemipelagic, have a low rate of sedimentation and are less likely to be influenced by turbidity and contour current (Wei et al., 2007; Gopalakrishnan et al., 2020; Govil et al., 2022). The sediment composition differs from that of the Bengal fan, which is dominated by marine biomass and terrestrial materials. It is generally understood that the terrestrial material of the NER should have come from the Bengal fan to the north, but is this really the case? Controversies remain regarding the provenance and transport route of the terrestrial materials in the NER (Bastia et al., 2010; Joussain et al., 2016; Li et al., 2017). Terrigenous materials are an important part of marine sediments and can be transported to the sea *via* mechanisms such as rivers and ocean currents. If the terrigenous material from the Himalayas cannot reach the NER through the Bengal Fan, does the terrigenous material of the NER come from the Qinghai-Tibet Plateau, and if so, what is the mode of transport? The clay mineral composition, particle size and radioisotope composition of the sediments can reflect their provenance, and the sedimentary source and transport route can be determined from that information (McLennan, 1989). This study attempts to identify the source and transport route of terrestrial sediments in the northern portion of the NER based on the clay mineralogy, Sr-Nd isotopes, grain size and the AMS ^{14}C of 77 seafloor surface sediments and three sediment cores recovered from the region. Additionally, this paper discusses the spatial and temporal variability recorded by the sediments over the past 35000 years. These results will provide an important reference for future studies of the marine palaeoenvironment, climate change and the relationship between the two and the Qinghai-Tibet Plateau.

2 Geological and oceanographic setting

The NER is located in the northeast Indian Ocean and is named after a series of seamount chains along the 90° E longitude line (Figure 1). The ridge is about 5,000 km long from north to south and 185 - 450 km wide from east to west. It is 1,000 to 3,500 meters above the ocean floor and lies 2,000 to 2,500 meters below the surface of the sea (Figure 1C). The NER is bounded by the Bengal Fan to the north, the Andaman Sea to the east, and Sri Lanka to the west. According to the 22 and 26 voyages data of the Deep Sea Drilling Program (DSDP) and the paleomagnetic data, the NER is the product of the Kerguelen hotspot during the late Cretaceous period when the Indian plate was rapidly drifting northward (Peirce, 1968; Curray et al., 1982). The Ar^{40}/Ar^{39} dating data show that the formation age of NER decreases from north to south from 84 Ma to 37 Ma, which indirectly supports the conclusion that the ridge originates from hotspots (Pringle et al., 2002). The bottom of the NER is basalt, and its upper part is composed of calcareous ooze of pelagic and semi-pelagic pelagic deposits, as well as some terrestrial materials.

The Bengal fan to the north of the NER is located at the eastern margin of the Indian plate, which is a collisional subduction zone where the Indian plate is subducted to the Eurasian plate (Figure 1). The Bengal fan belongs to a semi-closed marine environment and is the largest sedimentary fan in the world. It extends from 20°N to 10° S, is nearly 3,000 km long, 1,500 km wide, and covers an area of about $3\times10^6 km^2$. The water depth of the Bengal fan is 2000-4000 meters, it is deeper in the south, and the sediment thickness in the south is more than 10,000 meters (Stow, 1990). The fan sediments mainly come from the Himalayas and the Qinghai-Tibet Plateau and are transported through the Ganges River, the Yarlung Zangbo River, the Irrawaddy River, etc (Figure 1B). Turbidite deposition is apparent, and the provenance and transportation pathways of the sediments within the fan remains relatively constant (Fang et al., 2001, Fang et al., 2002; Phillips et al., 2014; Banerjee, 2018).

3 Materials and methods

3.1 Sample source

77 surface sediment samples and three core samples, A6, A28 and A34, were used in this analysis. The samples were recovered from the NER during the 2019 and 2020 voyages of the South China Sea Bureau of the Ministry of Natural Resources (see Figure 1 for the locations of the sampling points).

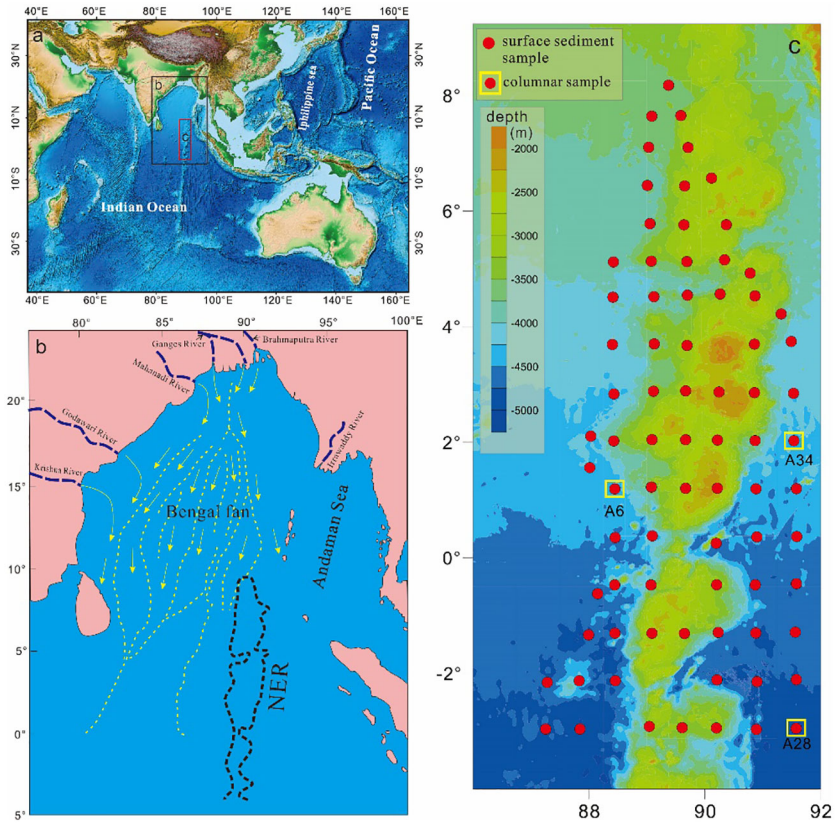

FIGURE 1
Location of the study area **(A)**, the source material of Bengal fan **(B)** and sample distribution **(C)**.

3.2 Particle size analyses

Particle size analyses were conducted on the three core samples. The pretreatment process was as follows: an appropriate amount of sediment was extracted every 1 cm downcore, 15 ml of 30% hydrogen peroxide was added, and the samples were allowed to stand for 24 h to remove any organic matter. Once the reaction was complete, approximately 5 ml of 3 M HCl were added to the samples which were then left for 24 h to acidify carbonate material. After the reaction was completed, the samples were centrifuged and then sonicated to mix the remaining sedimentary particles. Grain size was then measured in the School of Marine Science, Sun Yat-sen University by a Beckman Coulter (LS13320) laser diffraction particle size analyser with an analytical range of 0.4-2000 μm. The relative error of repeated measurements was less than 3%.

3.3 Sr-Nd isotope analysis

The Sr-Nd isotopes were measured from all of the 77 surface samples and the three sediment cores. After drying, grinding and sieving, the samples were sent to Nanjing FocuMS Technology Co. Ltd. for measurement of the Sr-Nd isotopic ratios. The organic carbon and carbonate in the sediments were removed by H_2O_2 and acetic acid, and then the samples were digested with concentrated HNO_3 and HF. The sample solution was eluted by a Biorad AG50W-X8 cation exchange column, then the matrix elements and Rb were removed by 2.0mol/L HCl, then the Sr components were received by leaching with 2.5mol/L HCl, and finally the total rare earth components were received by leaching with 6.0mol/L HCl. The SR component of the previous step was further purified by SR special resin. In the purification of Nd, Sm and Nd were separated by LN exchange column. The internal calibration ratios used for mass fractionation during the analysis were, $^{86}Sr/^{88}Sr$ = 0.1194 and $^{146}Nd/^{144}Nd$ = 0.7219. NIST SRM 987 and Nd isotope JNDI-1 were used as external calibration standards to account for instrument drift.

3.4 Clay mineral analysis

Qualitative tests of clay minerals were carried out on the sediments of A6, A28 and A34 at different downcore depths. Pretreatment before testing was done according to the following procedure (Liu et al., 2003; Trentesaux et al., 2003). To separate and extract the clay minerals, first dry a sample of the sediment, add a specific proportion of distilled water for soaking and rinsing, let stand, and remove the supernatant. Next add more distilled water, stir to suspend the sediment, let stand, and get a certain volume of the suspension. Due to the low clay mineral content of the samples, repeat the extraction process as needed. Once the suspension settles and the supernatant is removed, the remaining mud is the clay

material needed for the analysis. Transfer the mud into the drying oven at 60 °C for 12 h. Once dry, grind the sample into a powder. Finally, sift the samples through a 2 μM sieve to concentrate the clay minerals. Saturate the samples with ethylene glycol for 24 hours at room temperature. Then heat the samples at 490°C for 2 h. Once the samples had been properly prepared, they were subjected to three X-ray powder diffraction (XRD) runs. XRD patterns were obtained using a d/max 2500 PC diffractometer with CuK radiation at a voltage of 40 kV and a current intensity of 100 Ma. Diffraction patterns (2θ) were scanned from 5° to 30° in steps of 0.02°. The mineral composition was identified by jade software and the PDF2 database.

3.5 AMS ^{14}C analysis

Accelerator mass spectrometry (AMS) ^{14}C dating analyses for the three sediment cores were done in the Beta laboratory, and the results were corrected for $\delta^{13}C$ fractionation to obtain the conventional radiocarbon age. The experimental process was as follows: Appropriate amount of sediment samples were placed in a clean beaker, dried at 50°C, appropriate amount of mill - Q water was added, and the samples were fully soaked to disperse completely. Then transfer the sediment samples to a 63 μm stainless steel sieve and rinse samples under distilled water. Brush lightly with a brush until the sample is completely rinsed. Transfer the remaining sample in the sieve to a small beaker for drying and weighing. The uniform size of the foraminiferan G. menardii shells were selected under a solid microscope, and 3% H_2O_2 was added to remove the organic matter. After ultrasound, the turbidities were removed and the samples were dried. Finally, the G. menardii shell was collected into the plastic pipe and was performed ^{14}C dating on Ac ▪ celerator Mass Spectrometry (AMS) in Beta laboratory. The conventional radiocarbon ages were then calibrated with CALIB 7.2 software using a marine calibration curve to account for the marine reservoir effect (Liu et al., 2016a) and to convert the ages into the correct calendar age.

4 Results and analysis

4.1 Particle size analysis

We analysed the lithology of three sediment cores by particle size analyse experiments (Figure 2).

Core A6: The core is about 28 cm long. The colour of the sediment core is black from 1-2 cm, brown from 2 ~ 17 cm and gradually transitioning to black from 17 ~ 28 cm. The particle size measurement results show that the median particle size of the core varies from 6 to 48 μm, and the mean particle size is from 21.2 to 70.6 μm. The sediment composition of the core is clay and silty mudstone with clay minerals (<4 μm) and silty sand (4 ~ 63 μm) were 26.4% and 54.5%, respectively. The proportion of sand is less, the average content with sand size (> 63 μm) is 19.1%. The proportion of clay minerals decreased gradually from the bottom to the top of the core, while the sandy sediment showed an increasing trend. The average and median particle size suddenly increased at a depth of 9 ~ 10 cm (Figure 2).

Core A28: The core is about 45 cm long. The colour of the sediment core is white with a little black mixed in 1 ~ 3 cm, black on top and gradually lightened down to brown in 3 ~ 45 cm. The median particle size of the core is 21.4 ~ 73.6 μm, and the mean particle size is 39.6 ~ 96.1 μm. The sediment composition of the core is clay and silty mudstone with clay minerals (< 4 μm) and silty sand (4 ~ 63 μm) are 11.5% and 50.8%, respectively. The proportion of sand is larger than that of clay, and the average content with sand size (> 63 μm) is about 37.7%. The proportion of clay minerals increases gradually from the bottom to the top of the core, while the proportion of sandy sediments decreases.

Core A34: The core is about 40cm long. The colour of the sediment core is dark grey in 1 ~ 9 cm and brown in 9 ~ 40 cm. The median particle size of the core ranges from 5.1 to 10.3 μm, and the mean particle size varies from 15.1 to 48.1 μm. The sediment composition of the core is clay and silty mudstone with clay minerals (< 4 μm) and silty sand (4 ~ 63 μm) are 36.1% and 51.9%, respectively. The proportion of sand is less than that of clay, the average content with sand size (> 63 μm) is about 20%. The proportion of clay minerals in the core increases gradually from the bottom to the top of the core, while the proportion of sandy sediment decreases. The core contains a sudden increase in average and median particle size at a depth of 28 ~ 29 cm.

4.2 Sr-Nd isotopes and clay minerals

The Sr-Nd isotopic ratios for the 77 surface samples from the study area (Table 1, the duplicate sites in this table are two groups of parallel data, and the first data is used in mapping) show that the $^{87}Sr/^{86}Sr$ value ranges from 0.70919 to 0.71042, with an average value of 0.70951. This is close to the Sr isotope ratio of seawater (0.70924) and higher than the 0.7025 Sr isotope value for MORB (mid-ocean ridge basalt) (Goldstein et al., 1988). $^{144}Nd/^{143}Nd$ values ranged from 0.512042 to 0.512270, with an average of 0.512165, corresponding to ϵ Nd values. The ϵ Nd value varies from -11.631990 to -7.172703, with an average value of -9.238031, which is similar to that in the Indian Ocean ϵ Nd (- 7 ~ - 9) (Deng et al., 2012). Overall, the changes in isotopic ratios occur within a small range, with a positive ($^{87}Sr/^{86}Sr$) value and a negative ϵ Nd value.

The Sr-Nd isotope ratio results of the cores from the three NER stations, A6, A28 and A34, show that the core sediments and $^{144}Nd/^{143}Nd$ values vary little with depth. The $^{87}Sr/^{86}Sr$ ratio values fall between 0.7094321 and 0.7117061, with an average of 0.709937. The ratios of $^{144}Nd/^{143}Nd$ show minimal variability between 0.5121194 and 0.5122696, with an average of 0.512197, corresponding to the ϵ Nd range of -10.116300 to -7.1863576 (Table 2). The Sr-Nd ratio from the cores is similar to that of the surface samples, but the $^{87}Sr/^{86}Sr$ and $^{144}Nd/^{143}Nd$ ranges are slightly greater for the surface samples.

The analysis of mineral components less than 2 μM in cores A6, A28 and A34 of core samples shows that the main diffraction peaks are obvious in the measurement curves of natural slices of clay

10.3389/fmars.2023.1073054

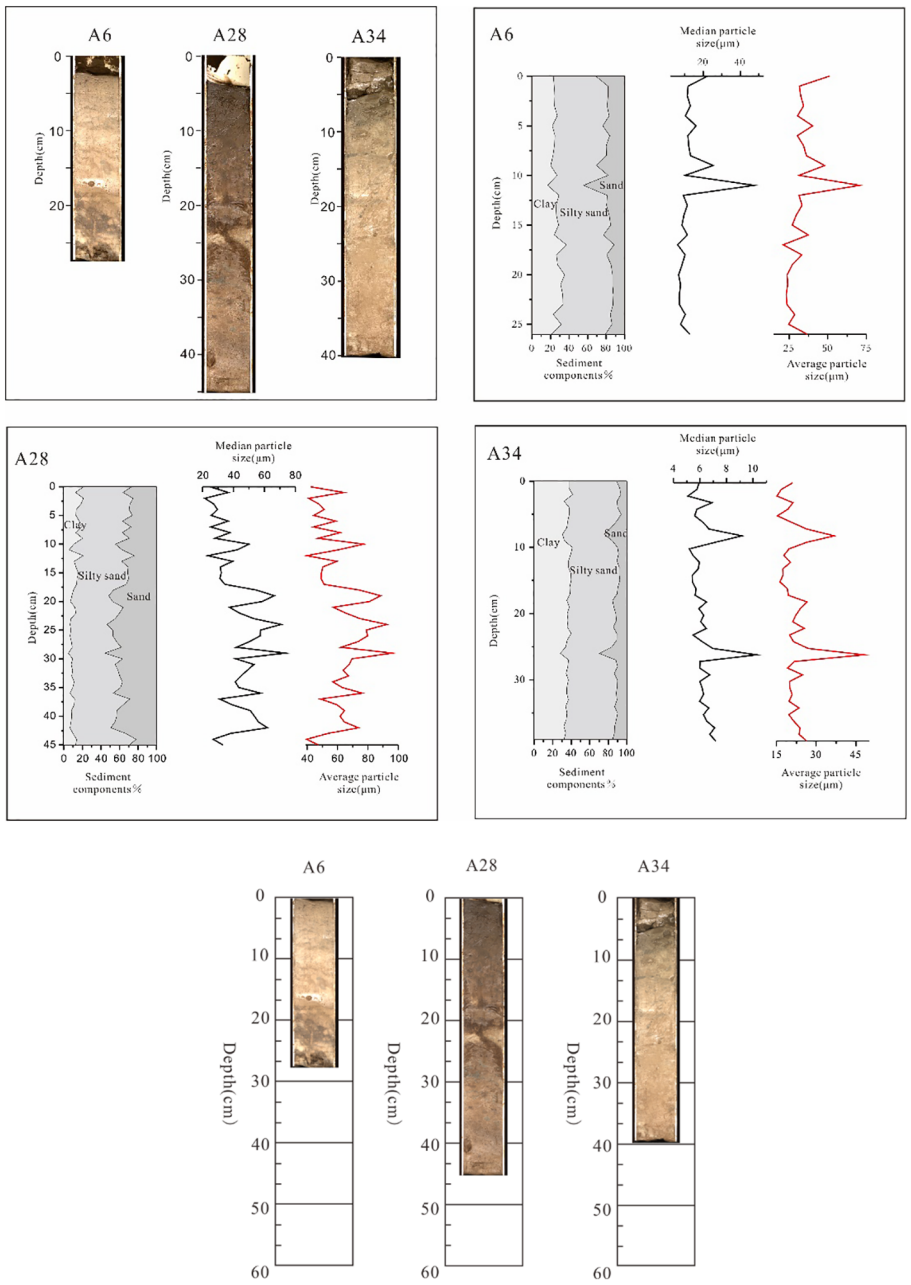

FIGURE 2
The sediment composition and particle size variability over core depth for A6, A28 and A34 cores.

minerals, and it can be identified that the components are mainly montmorillonite, illite, kaolinite, chlorite and a small amount of quartz, of which illite is the main component, chlorite and kaolinite are the second, and the diffraction peaks of montmorillonite are not obvious (Figure 3).

4.3 Chronological analysis

^{14}C enters marine sediments after a series of long-term cycles and decays at a constant rate (half-life: 5730 years). In the sedimentary layer, when the burial depth increases, the ^{14}C index decreases (Zhang and Zhou, 2012). The maximum age of the three sediment cores in the study is 35000 years before present, and the overall sedimentation rate is low, with an average of 1 cm ka^{-1} (Table 3). The deposition rate accelerated at 12 ~ 18 ka Bp. The deposition rate of core A28 peaked at 25 cm ka^{-1}, but was followed by an extremely rapid decrease (Figure 4). Visual analysis of the core showed that the sediment colour at this interval (19 ~ 20 cm depth) is significantly darker, represented by a dark sediment layer as shown by Figure 2. This abrupt change in the rate of sediment deposition corresponds to the Younger Dryas (12.9 ~ 11.5 ka BP).

10.3389/fmars.2023.1073054

TABLE 1 Summary statistics for Sr-Nd isotope ratios of surface samples of the northern NER and compared adjacent regions.

Areas	Statistics	$^{87}Sr/^{86}Sr$	$^{143}Nd/^{144}Nd$	εNd
NER (This paper)	Sample quantity	77	77	77
	Minimum value	0.7091881	0.512042	-11.6319898
	Maximum value	0.7104238	0.512270	-7.1727027
	Average value	0.7095103	0.5121645	-9.2380319
	Standard deviation	0.0003168	0.0000489	0.9540171
UCC (DePaolo, 1988)			0.5119	< - 6
Northern of Bay of Bengal (Colin et al., 1999)	Sample quantity	6	6	6
	Minimum value	0.71453	0.511981	-12.8
	Maximum value	0.72587	0.512277	-7
	Average value	0.72011	0.512102	-10.45
	Standard deviation	0.0038778	0.0001061	2.0750502
Western of Bay of Bengal (Colin et al., 1999)	Sample quantity	4	4	4
	Minimum value	0.72305	0.511809	-16.2
	Maximum value	0.73156	0.511924	-13.9
	Average value	0.72612	0.5118525	-15.325
	Standard deviation	0.0032859	0.0000472	0.9283722
Eastern of Bay of Bengal (Andaman Sea) (Colin et al., 1999)	Sample quantity	23	23	23
	Minimum value	0.71232	0.511998	-12.5
	Maximum value	0.72230	0.512209	-8.4
	Average value	0.716263	0.512120	-10.1
	Standard deviation	0.0026210	0.0000536	1.0459030
Irrawaddy River (Colin et al., 1999)	Sample quantity	3		3
	Minimum value	0.7118		-7.3
	Maximum value	0.7120		-6.8
	Average value	0.7119		-7
	Standard deviation	0.0000816		0.2160247
Godavari-Krishna River (Ahmad et al., 2009)	Sample quantity	3		3
	Minimum value	0.724		-16.38
	Maximum value	0.725		-12.38
	Average value	0.7244888		-14.38
	Standard deviation	0.0004082		1.6329931
Gangas (Lupker et al.,2013)	Sample quantity	21		21
	Minimum value	0.757574		-18.8
	Maximum value	0.801759		-17.3
	Average value	0.774910		-18.0
	Standard deviation	0.0098453		0.3740445
Brahmaputra (Lupker et al.,2013)	Sample quantity	9		9
	Minimum value	0.721437		-19
	Maximum value	0.754689		-14.2

(Continued)

TABLE 1 Continued

Areas	Statistics	$^{87}Sr/^{86}Sr$	$^{143}Nd/^{144}Nd$	εNd
	Average value	0.739170		-16.8
	Standard deviation	0.0125933		1.7239776
Lower Meghna (Lupker et al.,2013)	Sample quantity	9		9
	Minimum value	0.72322		-17
	Maximum value	0.746403		-13.7
	Average value	0.736937		-15.8
	Standard deviation	0.0078554		1.0343484
Andaman mud volcanoes (Lupker et al.,2013)	Sample quantity	14	14	14
	Minimum value	0.70854	0.51247	-3.3
	Maximum value	0.70986	0.512552	-1.7
	Average value	0.70924	0.512505	-2.6
	Standard deviation	0.0003586	0.0000233	0.4533323

5 Discussion

5.1 Provenance tracing

The Sr-Nd isotopes have a long half-life and can maintain relative stability as they undergo various geological processes (Huang et al., 2005). These isotopes have become a good tracer for determining sediment sources. It is generally believed that when the $^{87}Sr/^{86}Sr$ ratio in the sediment is > 0.710, the material source is considered to be from the crust; when $^{87}Sr/^{86}Sr$ is < 0.705, the material likely originated from the mantle (Fang et al., 2020). $^{143}Nd/^{144}Nd$ in the continental Erosion Products = 0.51204 ± 0.0002(ϵ Nd = − 11.4 ± 4), and the $^{143}Nd/^{144}Nd$ ratio of continental crust is close to 0.5119 (DePaolo, 1988; Goldstein et al., 1984). Therefore, sediments flowing through older crustal rocks usually have higher $^{87}Sr/^{86}Sr$ ratios and lower εNd values (< -6) (De Paolo and Johnson, 1979), such as the low εNd values (-14 to -15) and the high $^{87}Sr/^{86}Sr$ ratio (0.710 to 0.714) of the North China Dabie complex, that indicates the hybridization of the ancient crust (Jahn et al., 1999).

The obvious differences between different rivers around the Bay of Bengal make it a good location to trace sediment sources (Galy and France-Lanord, 1999; Kessarkar et al., 2005; Tripathy et al., 2014; Joussain et al., 2016). By analysing the Sr-Nd isotope ratios, the εNd values previously obtained from the river sediments around the Bay of Bengal, and the corresponding marine sediments, it is found that the distribution of Sr-Nd isotopes in the marine sediments is consistent with the potential terrigenous source of the river system that transport materials into these areas (Tripathy et al., 2011). For example, the $^{87}Sr/^{86}Sr$ value of the Eastern Bay of Bengal (Andaman Sea) is 0.712~0.722, which is close to the $^{87}Sr/^{86}Sr$ value of the middle Irrawaddy River (Colin et al., 1999), while the $^{87}Sr/^{86}Sr$ value of marine sediments in the west of the Bay of Bengal is 0.723~0.732, which is similar to the $^{87}Sr/^{86}Sr$ value of sediments in the Godavari River on the central and western coasts (Colin et al., 1999; Ahmad et al., 2005; Ahmad et al., 2009; Chaitanya et al., 2021).

Our Sr-Nd isotope test results (Tables 1 and 2) show that the surface sediments of the NER and the sediments from the three sediment cores all have low εNd values (- 11.631990 to -7.172703)

TABLE 2 The Sr-Nd isotope ratios of some core sediments in the NER.

Site	Depth (cm)	$^{87}Sr/^{86}Sr$	$^{143}Nd/^{144}Nd$	εNd
A6	1-2	0.7094493	0.5121729	-8.703998
A6	12-13	0.7094321	0.5121918	-8.173409
A6	26-27	0.7095701	0.5122190	-7.213667
A28	1-2	0.7117061	0.5122217	-7.186358
A28	22-23	0.7096804	0.5122682	-9.930984
A28	45-46	0.7095537	0.5122696	-8.87956
A34	0-1	0.7102207	0.5121194	-9.072679
A34	19-20	0.7098994	0.5121289	-8.12074
A34	39-40	0.7099192	0.5121828	-10.1163

10.3389/fmars.2023.1073054

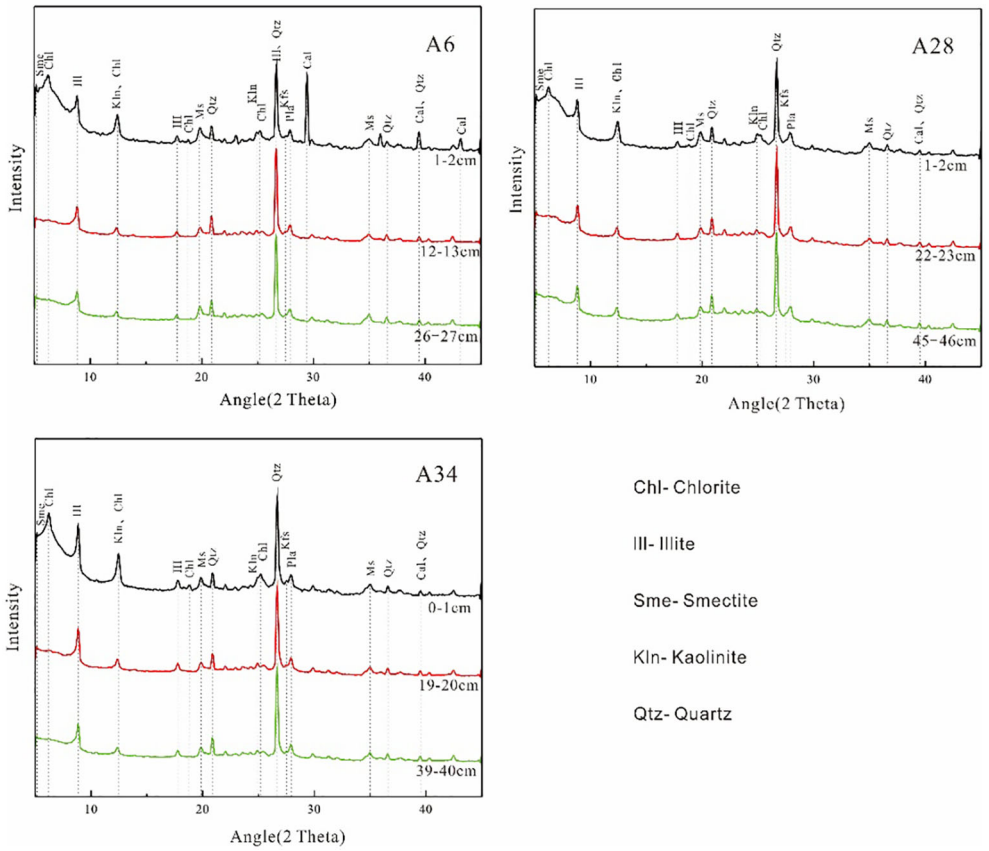

FIGURE 3
Diffraction spectrum of clay minerals in core sediments from stations A6, A28 and A34.

TABLE 3 AMS ^{14}C age data from A6, A28 and A34 cores.

Site	Depth/cm	**14C** age **(a B.P.)**	Calibrated radiocarbon age (cal a BP)		Rate of sedimentation (cm. ka^{-1})
			median/(a BP)	1σ	
A6	2	4750 ± 30	4797.5	4975-4620	0.63
	9	9740 ± 30	10483	10668-10298	1.27
	18	13210 ± 40	15050.5	15265-14836	1.98
	25	15600 ± 40	18041.5	18245-17838	2.34
A28	12	11430 ± 30	12769	12906-12632	1.02
	19	11740 ± 30	13052	13206-12898	24.73
	30	13180 ± 40	15017.5	15233-14802	5.6
	43	31370 ± 160	34944	35324-34564	0.65
A34	1	4580 ± 30	4608	4786-4430	0.43
	28	12070 ± 40	13399.5	13565-13234	1.88
	37	16460 ± 50	18973.5	19202-18745	1.61

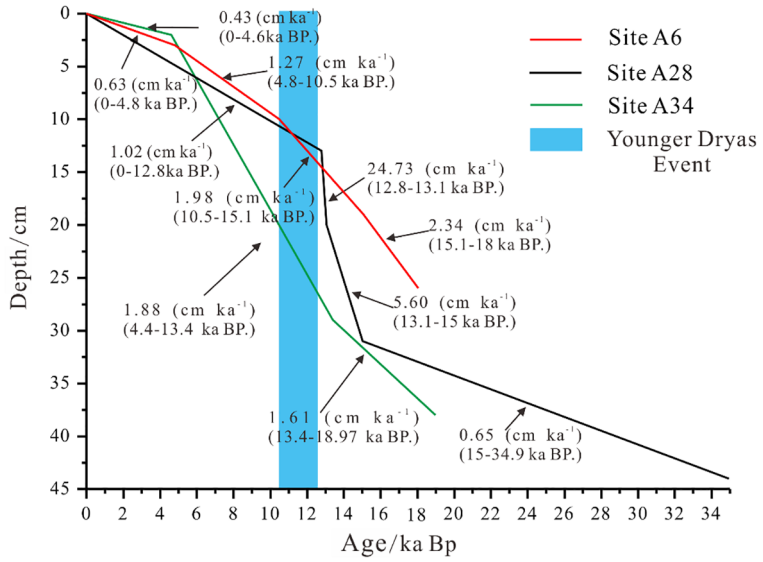

FIGURE 4
Depth versus calibrated calendar age plot of A6, A28 and A34 cores. The linear sedimentation rates are listed for each interval in cm ka^{-1}.

and high $^{87}Sr/^{86}Sr$ ratios (0.70919 to 0.71042), indicating that their source rocks contain a large amount of ancient crustal materials.

The average value of $^{87}Sr/^{86}Sr$ of the surface sediments obtained from the NER is 0.7095, and the average value of $^{143}Nd/^{144}Nd$ is 0.5122, indicating that a large number of diagenetic materials in the sediments come from continental crust sources and have been eroded. It can be seen from the correlation distribution diagram of εNd and $^{87}Sr/^{86}Sr$ (Figure 5) that the $^{87}Sr/^{86}Sr$ values of the surface sediments and the core sediments are very close to the $^{87}Sr/^{86}Sr$ range of 0.712~0.719 (Colin et al., 1999), indicative of the Irrawaddy River, whose provenance is the Qinghai Tibet Plateau. These values are also similar to the value of the Eastern Bay of Bengal (Andaman Sea) (Figure 5). The average value of εNd for the surface sediment in the study area is -9.238, which is also within the range of the Irrawaddy River (- 6.9 ~ 10.86) (Figure 5). Only a small amount of surface sediments have εNd and $^{87}Sr/^{86}Sr$ values suggestive of an origin in the Ganges Brahmaputra River system close to the northern and southern foothills of the Himalayas.

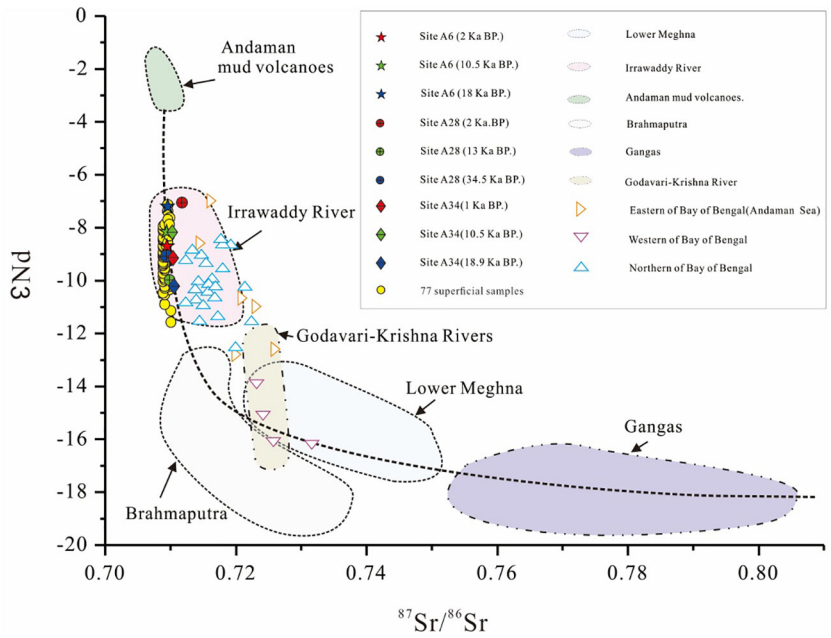

FIGURE 5
Correlation distribution diagram of εNd and $^{87}Sr/^{86}Sr$ in the sediments of the NER and the Bay of Bengal and its surrounding rivers.

The research method of Sr-Nd isotopes combined with clay mineral analysis is widely used. The fine-grained, clay dominated sediments are mainly transported by rivers, and there are obvious differences in the clay mineral composition representative of potential sources. Therefore, the study of clay composition within fine-grained sediments can be used as important evidence to determine sedimentary sources and transport pathways (Ahmad et al., 2012; Liu et al., 2016b). On the other hand, the formation and diagenesis of clay minerals are closely related to the environment in which they are located, and the effects of these processes may be reflective of local environmental conditions (Tang et al., 2002).

Various sediment inlets in the Northeast Indian Ocean have different clay mineral assemblages. The clay minerals in the surface sediments of the southeastern Andaman Sea are mainly composed of illite (45%), kaolinite (31%), chlorite (18%), and smectite (6%) (Cao, 2015). The sediments of the Mahanadi River are characterized by high illite content and low montmorillonite content (Li et al., 2018). The clay mineral contents in the sediments of the Ganges-Brahmaputra River system are illite (57%), kaolinite, chlorite and montmorillonite (less than 5%) from high to low (Khan et al., 2019). The sediment in the offshore basin near the Krishna-Godavari estuary has a high content of montmorillonite and a low content of chlorite (Phillips et al., 2014). Although the runoff and sedimentary input of the Ganges-Brahmaputra-Meghna River system is much larger than that of other basins (Milliman et al., 1983), Himalayan materials from the Irrawaddy River and Yarlung Zangbo River are more important and stable sources (Song et al., 2021). Illite is the predominate material in the clay mineral composition of the NER, followed by chlorite and kaolinite. Montmorillonite is the least abundant (Figure 3). The clay mineralogy of the NER is similar to that of the surface sediments of the Andaman Sea, indicating a shared provenanced, though small inputs from the Ganges Brahmaputra River and Mahanadi River affect the sedimentary source.

To summarize the Sr-Nd isotope and clay mineral analysis, the sediments in the study area contain a large amount of older continental crust materials from the Qinghai-Tibet Plateau, which have been subjected to certain erosional processes and may have been imported to the NER *via* the Irrawaddy River and the Andaman Sea.

5.2 Distribution of surface sediments on the NER

A large volume of surface sediments encompassing a wide area were collected in the NER. The Sr-Nd isotope test results can not only be used for provenance tracing but also to study the distribution pattern of terrestrial material after it enters the study area. The distribution of the εNd (0) value and $^{87}Sr/^{86}Sr$ isotope ratios of surface sediments are an important indication of the current source input pathways. By analysing the Sr-Nd isotope distribution characteristics of 77 surface samples obtained from the NER, we found that the $^{143}Nd/^{144}Nd$ isoline map (Figure 6A) showed that the values decreased from south to north. The $^{87}Sr/^{86}Sr$ contour map (Figure 6B) shows a decreasing trend from east to west.

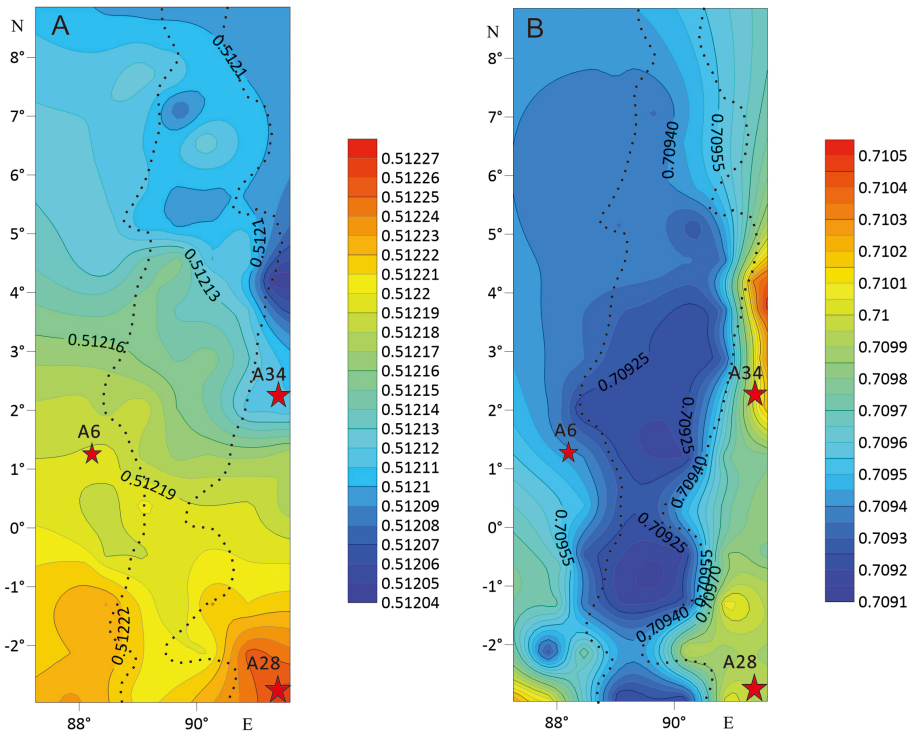

FIGURE 6
$^{143}Nd/^{144}Nd$ contour map **(A)** and $^{87}Sr/^{86}Sr$ contour map **(B)** in the study area. (Note: The dotted line represents the position of NER, and the asterisk represents the core sample position).

Sedimentation has little influence on Nd and its ratio in sediments. Nd isotopes can effectively identify and trace terrigenous sedimentary materials and indicate their evolutionary history (Shao et al., 2009). The εNd value of the materials imported into the sea from the land is smaller than that of marine biomass (Liu, 2004). According to the distribution pattern that the $^{143}Nd/^{144}Nd$ ratio in the study area gradually increases from north to south, it is inferred that the material sources are mainly transported from north to south. The larger the ratio of $^{87}Sr/^{86}Sr$ is, the older the sediments and the greater the chemical weathering (Meng et al., 2000). As the $^{87}Sr/^{86}Sr$ value decreases from east to west, the chemical weathering in the east of the NER is greater than that in the west. This may be because the monsoon weakens after it passed through the ridge, the hydrodynamic effect of the seawater carrying terrestrial materials was weakened, thus reducing its ability to further transport sediments from east to west. Therefore, the migration mode of the sediment transported to the NER is from east to west and from north to south.

5.3 Sediment transport mode and its temporal and spatial changes

The NER is relatively high and located in the open ocean far from the source area. Turbidity currents and isobaric currents have little impact on it. The isotope and clay mineral analysis results show that the winter monsoon and summer monsoon in the Bay of Bengal can transport the terrigenous sediments of the northern mountain system to the northern end of the NER (Wei et al., 2007; Zhang et al., 2007; Weber et al., 2018), but it is difficult to transport them further southward. However, after the sediments exported from the Irrawaddy River flow through the relatively closed Andaman Sea *via* the summer monsoon, the monsoon-driven circulation in this area can be used to transport more sediments to the northern NER (Schott and McCreary, 2001; Shankar et al., 2002; Joussain et al., 2016). This interpretation is supported by the observed decrease in $^{143}Nd/^{144}Nd$ and $^{87}Sr/^{86}Sr$ values from northeast to south and east to west, as shown in the isotope contour maps (Figure 6).

Therefore, we comprehensively analysed the Sr-Nd isotopes and their spatial distribution and clay mineralogy in the study area and proposed the following transport mode of terrigenous materials into the NER. In the Qinghai-Tibet Plateau, a large volume of continental crust materials was weathered and denuded and then transported into the Irrawaddy River. Terrigenous clastic materials were carried to the Andaman Sea with the flowing waters of the Irrawaddy River. It is transported westward to the north of the NER through the surface monsoon circulation of the Andaman Sea. Under the influence of the monsoon circulation in the study area, the terrigenous materials continue to be carried southward along the NER (Figure 7), and the Sr-Nd ratio remains relatively stable along the entire transport path.

To explore the temporal and spatial changes in this transport mode of sediments to the NER, we performed AMS ^{14}C dating analysis on three core sediments.

The maximum ages of the A6, A34 and A28 cores are 18ka, 19ka and 35ka respectively. A6 and A34 cores in the northern part of the NER recorded the sedimentary and environmental changes

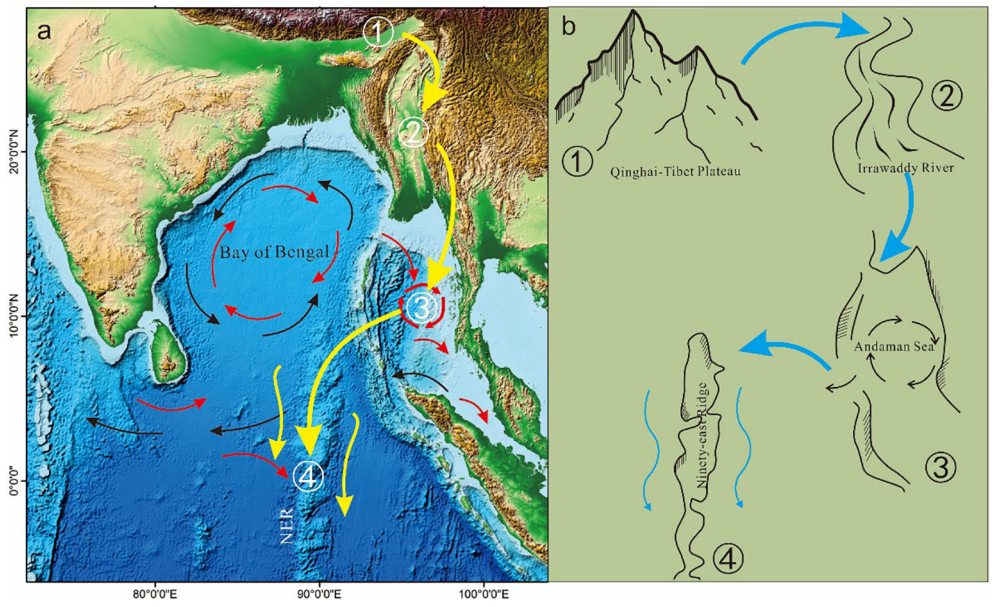

FIGURE 7
Transport path pattern of terrigenous sediments in the NER. **(A)** and migration model from the Qinghai - Tibet Plateau to the NER **(B)**. (**A**: black arrow indicates winter monsoon, red arrow indicates summer monsoon, yellow arrow indicates transport path, cited by Joussain et al, 2016; **A, B**: ①- Weathering and denudation of the Qinghai-Tibet Plateau;②- Material from the Qinghai-Tibet Plateau was transported to the Irrawaddy River; ③- Material from the Tibetan Plateau drains into Andaman Sea, and then enters monsoon circulation system; ④- Material from the Tibetan Plateau are transported westward to the northern NER by the monsoon-driven circulation.).

after the last glacial maximum (LGM, 26.5 ka ~ 19 ka BP), including the Younger Dryas (12.6 Ka ~ 11.5 ka BP). The two cores reflect similar sedimentation rates, and there is no significant change during the Younger Dryas (12.6 Ka ~ 11.5 ka BP). After the Younger Dryas (12.6 Ka ~ 11.5 ka BP), the sea level rose and the sedimentation rates began to decrease, suggesting that the northern part of the NER may be mainly affected by sea level changes. The deposition of A28 core in the southern NER records the sedimentary and environmental changes since the late period of the last glacial period (70 ka ~ 11.5ka BP), including the LGM and the Younger Dryas. AMS ^{14}C dating analysis of the core shows that the sediments in the southern NER were stable from 35ka BP to 15ka BP and were not affected by the LGM, indicating that the southern NER was not affected by provenance and sea level during this period. From 15ka BP to 12.6ka BP (before the Younger Dryas), A sudden increase in the sedimentation rate in the southern NER could be linked to a number of factors. The first factor may be that as the climate warms, the increase of provenance denudation and stream input amount during this period (Kolla and Pierre, 1973; Kolla et al., 1976). And the second reason may be that large amounts of volcanic material from the Indonesian archipelago were deposited, carried by the southeast monsoon or equatorial easterly winds (Dehn et al., 1991; Hovan and Rea, 1992; Zhang et al., 2004). Since the Younger Dryas (12.6ka BP), the sedimentation rate of the southern NER decreased, which may be affected by the decrease of provenance denudation and the stream input amount.

We also found that the mean particle size of the A6, A28 and A34 cores are relatively uniform, but there is a sudden change in sedimentation during the period of rapid climate change (12.9 ~ 11.5 ka BP) in the Younger Dryas (Broecker et al., 2010; Liu, 2012). The deposition processes at the NER may also be affected by this climatic change. The Sr-Nd isotope values of the A28 and A34 core samples had obvious changes after the Younger Dryas, especially the εNd values, which decreased rapidly, confirming the change in source (Figure 8). Core A6, located west of the ridge, differs from the other two cores potentially due to their different locations (east of the ridge). However, A6 also contains evidence of a change at approximately 15 ka BP, after the Younger Dryas. In general, the sediment transport regime in the study area has been relatively stable for the past 35000 years and is essentially the same as the current model. However, during the Younger Dryas (12.9 ~ 11.5 ka BP), the quantity of sedimentary input, particle size and Sr-Nd isotope ratio changed. The relationship between this change and the climate of the Younger Dryas needs to be further studied.

6 Conclusion

1. The sediments of the NER contain a large volume of terrigenous materials. The sedimentary source is mainly the older continental crust of the Qinghai-Tibet Plateau and there is less terrigenous material transported directly from the Bay of Bengal in the north.
2. We propose a transport model of terrigenous sediments into the NER: In the Qinghai-Tibet Plateau, the crustal materials are weathered and denuded and then transported into the Andaman Sea *via* the Irrawaddy River. Then, under the influence of the summer monsoon, they are transported westward to the northern NER by the monsoon-driven circulation before finally being deposited further south.
3. This mode of terrigenous sediment transport into the NER has changed very little over the past 35000 years. Only during the rapid climate change of the Younger Dryas (12.9 ~ 11.5 ka BP) did the input amount, grain size and Sr-Nd isotope value of sediments show substantial change.

Data availability statement

The original contributions presented in the study are included in the article/Supplementary Material. Further inquiries can be directed to the corresponding author.

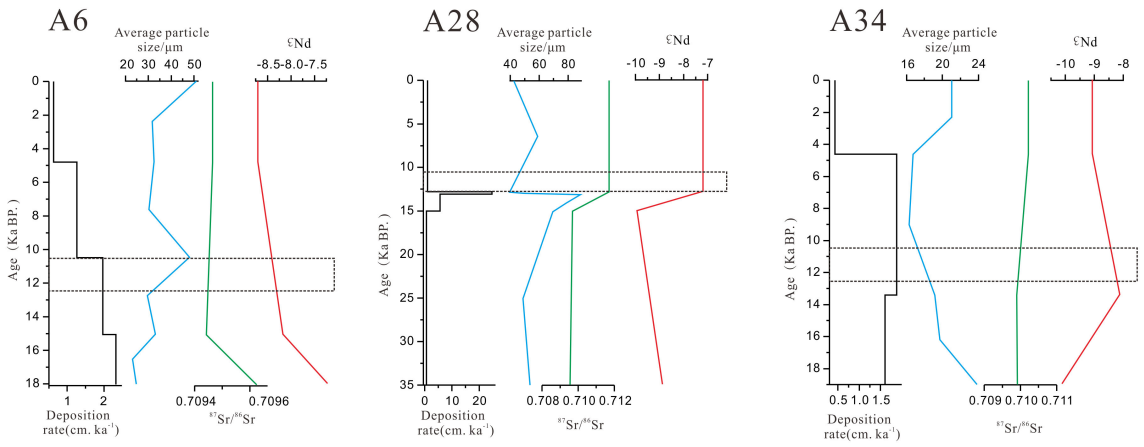

FIGURE 8
Chronological framework of sediments in A6, A28 and A34 cores (the middle of the dotted line is the Younger Dryas).

Author contributions

ZC - conception and design. QH - data analysis and writing. ZY - conception and sampling. XH - data analysis and writing. LC - revising the manuscript. MT - revising the manuscript. All authors contributed to the article and approved the submitted version.

Funding

This research was funded by National Programme on Global Change and Air-Sea Interaction (No. GASI-02-IND-CJ04), National Natural Science Foundation of China (No. 41206035) and Nature Science Foundation of Guangdong Province (No. 2015A030313157, No. 2107A030312002, 2018A030313168).

Acknowledgments

The samples were from the 2019 and 2020 voyages of the South China Sea Bureau of the Ministry of Natural Resources and the First Institute of Oceanography. The data of X Ray Fluorescence (XRF) core scanner were from Guangzhou Marine Geological Survey. The data of geochemistry were from Nanjing FocuMS Technology Co. Ltd. The data of grain size were from School of Marine Science of Sun Yat-sen University and the data of X-ray powder diffraction (XRD) were from the testing center of Sun Yat-sen University. Data sets and figures noted in the main text can be found in the main text.

Conflict of interest

The authors declare that the research was conducted in the absence of any commercial or financial relationships that could be construed as a potential conflict of interest.

Publisher's note

References

Agarwal, N., Sharma, R., and Kumar, R. (2022). Impact of along-track altimeter sea surface height anomaly assimilation on surface and sub-surface currents in the Bay of Bengal. *Ocean Model.* 169, 101931–. doi: 10.1016/j.ocemod.2021.101931

Ahmad, S. M., Anil Babu, G., Padmakumari, V. M., Dayal, A. M., Sukhija, B. S., and Nagabhushanam, P. (2005). Sr, Nd Isotopic evidence of terrigenous flux variations in the Bay of Bengal: Implications of monsoons during the last 34,000 years. *Geophys. Res. Lett.* 32 (22), L22711. doi: 10.1029/2005GL024519

Ahmad, S. M., Padmakumari, V. M., and Babu, G. A. (2009). Strontium and neodymium isotopic compositions in sediments from godavari, Krishna and pennar rivers. *Curr. Science: A Fortnightly J. Res.* 97 (12), 1766–1769. doi: 10.1098/rsta.2009.0182

Ahmad, S. M., Zheng, H., Raza, W., Zhou, B., Lone, M. A., Raza, T., et al. (2012). Glacial to Holocene changes in the surface and deep waters of the northeast Indian ocean. *Mar. Geology* 329/331, 16–23. doi: 10.1016/j.margeo.2012.10.002

Banerjee, B., Ahmad, S. M., Babu, E. V. S. S., Padmakumari, V. M., Beja, S. K., Satyanarayanan, M., et al. (2018). Geochemistry and isotopic study of southern Bay of Bengal sediments: Implications for provenance and paleoenvironment during the middle Miocene. *Palaeogeography Palaeoclimatology Palaeoecology: Int. J. Geo-Sciences* 514, 156–167. doi: 10.1016/j.palaeo.2018.10.022

Bastia, R., Das, S., and Radhakrishna, M. (2010). Pre- and post-collisional depositional history in the upper and middle Bengal fan and evaluation of deepwater reservoir potential along the northeast continental margin of India. *Mar. Petroleum Geology* 27 (9), 2051–2061. doi: 10.1016/j.marpetgeo.2010.04.007

Broecker, W. S., Denton, G. H., Edwards, R. L., Cheng, H., Alley, R. B., and Putnam, A. E. (2010). Putting the younger dryas cold event into context. *Quaternary Sci. Reviews: Int. Multidiscip. Rev. J.* 29 (9/10), 1078–1081. doi: 10.1016/j.quascirev.2010.02.019

Cao, P., Shi, X., Li, W., Liu, S., Yao, Z., Hu, L., et al. (2015). Sedimentary responses to the Indian Summer Monsoon variations recorded in the southeastern Andaman Sea slope since 26 ka. *J. Asian Earth Sci.* 114, 512–525. doi: 10.1016/j.jseaes.2015.06.028

Chaitanya, A. V. S., Vialard, J., Lengaigne, M., d'Ovidio, F., Riotte, J., Papa, F., et al. (2021). Redistribution of riverine and rainfall freshwater by the Bay of Bengal circulation. *Ocean Dynamics* 71 (11/12), 1113–1139. doi: 10.1007/s10236-021-01486-5

Clark, M. K., House, M. A., Royden, L. H., Whipple, K., Burchfiel, B. C., Zhang, X., et al. (2005). Late Cenozoic uplift of southeastern tibet. *Geology* 33 (6), 525. doi: 10.1130/g21265.1

Colin, C., Turpin, L., Bertaux, J., Desprairies, A., and Kissel, C. (1999). Erosional history of the Himalayan and burman ranges during the last two glacial-interglacial cycles. *Earth Planetary Sci. Letters: A Letter J. Devoted to Dev. Time Earth Planetary System* 171 (4), 647–660. doi: 10.1016/S0012-821X(99)00184-3

Curray, J. R., Emmel, F. J., and Moore, D. G. (2002). The Bengal fan: morphology, geometry, stratigraphy, history and processes. *Mar. Pet. Geol* 19 (10), 1191–1223. doi: 10.1016/S0264-8172(03)00035-7

Curray, J. R., Emmel, J. F., Moore, D. G., and Raitt, R. W. (1982). Structure, tectonics, and geological history of the northeastern Indian Ocean. *The ocean basins and margins: The Indian Ocean*, 399–450. doi: 10.1007/978-1-4615-8038-6_9

Dehn, J., Farrell, J. W., and Schmindke, H. U. (1991). "Neogene tephrochronotogy from Site758 on northern ninetyeast ridge: Indonesian arc volcanism of the past 5 ma," in *Proc.ODP sci. results*, vol. 121 . Eds. J. Weissel and J. Peirce, 273–293. doi: 10.2973/odp.proc.sr.121.123.1991

Deng, X. G., Yang, Y. H., Yang, Y., Yao, H. Q., and Wu, L. S. (2012). Mantle material source of sulfide in the mid-ridge contract area of southwest Indian: Sr-Nd-Pb isotopic evidence. *Mineral Deposits.* 31 (S1), 535–536. doi: 10.16111/j.0258-7106.2012.s1.271

De Paolo, D. J., and Johnson, R. W. (1979). Magma genesis in the new Britain island-arc: Constraints from Nd and Sr isotopes and trace-element patterns. *Contributions to Mineralogy Petrology.* 70 (4), 367–379. doi: 10.1007/BF00371044

DePaolo, D. J. (1988). Neodymium isotope geochemistry. an introduction. *Minerals and rocks* 20, 1–187. doi: 10.1180/minmag.1990.054.376.21

Durand, F., Shankar, D., Birol, F., and Shenoi, S. S. C. (2009). Spatiotemporal structure of the East India coastal current from satellite altimetry. *J. Geophys. Res.* 114, C02013. doi: 10.1029/2008JC004807

Fang, N. Q., Chen, X. F., Ding, X., Hu, C. Y., Yin, Y., and Nie, H. G. (2001). Paleoceanographical records under impact of the Indian monsoon from the Bengal deep Sea fan and ninetyeast ridge during the last 260 ka. *Sci. China Ser. D.* 44 (S1), 351–359. doi: 10.1007/BF02912006

Fang, N. Q., Chen, P., Lin, W. U., and Shi, F. (2002). Contour currents in deep-water records from Bay of Bengal and its environmental implication. *J. Earth Sci.* 27 (5), 570–575. doi: 10.3321/j.issn:1000-2383.2002.05.016

Fang, X., Song, Y., Tang, J. X., Wang, J. X., and Li, H. F. (2020). Metallogenic epoch study on the shangxu gold deposit, bangong-nujiang suture zone, Tibet and its geological implications. *Acta Geologica Sinica.* 94 (11), 3376–3390. doi: 10.3969/j.issn.0001-5717.2020.11.013

Galy, A., and France-Lanord, C. (1999). Weathering processes in the gangess–Brahmaputra basin and the riverine alkalinity budget. *Chem. Geology.* 159, 31–60. doi: 10.1016/S0009-2541(99)00033-9

Goldstein, S. L., O',Nions, R. K., and Hamilton, P. J. (1984). A Sm-Nd isotopic study of atmospheric dusts and particulates from major river systems. *Earth Planetary Sci. Lett.* 70, 221–236. doi: 10.1016/0012-821X(84)90007-4

Goldstein, S. L. (1988). Decoupled evolution of Nd and Sr isotopes in the continental crust and the mantle. *Nature* 336 (6201), 733–738. doi: 10.1038/336733a0

Gopalakrishnan, G., Subramanian, A. C., Miller, A. J., Seo, H., and Sengupta, D. (2020). Estimation and prediction of the upper ocean circulation in the Bay of Bengal. *Deep-Sea Res. Part II-topical Studies in Oceanography* 172, 104721. doi: 10.1016/j.dsr2.2019.104721

Govil, P., Mazumder, A., Agrawal, S., Azharuddin, S., Mishra, R., Khan, H., et al. (2022). Abrupt changes in the southwest monsoon during mid-late Holocene in the western Bay of Bengal. *J. Asian Earth Sci.* 227, 105100. doi: 10.1016/j.jseaes.2022.105100

Hall, R. (2002). Cenozoic Geological and plate tectonic evolution of SE Asia and the SW pacific: computer-based reconstructions, model and animations. *J. Asian Earth Sci.* 20 (4), 353–431. doi: 10.1016/S1367-9120(01)00069-4

Hovan, S. A., and Rea, D. K. (1992). The Cenozoic record of continental mineral deposition on broken and ninetyeast ridges, Indian ocean: Southern African aridity and sediment delivery from the Himalayas. *Paleoceanography* 7 (6), 833–860. doi: 10.1029/92PA02176

Huang, S. J., Wu, S. J., Sun, Z. L., Pei, C. R., and Hu, Z. W. (2005). Sea Water strontium isotopes and paleo-oceanic events over the past 260 ma. *Earth Sci. Front.* 12 (2), 133–141. doi: 10.3321/j.issn:1005-2321.2005.02.015

Jahn, B. M., Wu, F., Lo, C. H., and Tsai, C. H. (1999). Crust–mantle interaction induced by deep subduction of the continental crust: geochemical and Sr–Nd isotopic evidence from post-collisional mafic–ultramafic intrusions of the northern dabie complex, central China-ScienceDirect. *Chem. Geology*. 157 (1–2), 119–146. doi: 10.1016/S0009-2541(98)00197-1

Joussain, R., Colin, C., Liu, Z., Meynadier, L., Fournier, L., Fauquembergue, K., et al. (2016). Climatic control of sediment transport from the Himalayas to the proximal NE Bengal fan during the last glacial-interglacial cycle. *Quaternary Sci. Reviews: Int. Multidiscip. Rev. J.* 148, 1–16. doi: 10.1016/j.quascirev.2016.06.016

Kessarkar, P. M., Rao, V. P., Ahmad, S. M., Patil, S. K., Kumar, A. A., Babu, G. A., et al. (2005). Changing sedimentary environment during the late quaternary: Sedimentological and isotopic evidence from the distal Bengal fan. *Deep-sea research Part II. Topical Stud. oceanography* 52 (9), 1591–1615. doi: 10.1016/j.dsr.2005.01.009

Khan, M. H. R., Liu, J., Liu, S., Seddique, A. A., Cao, L., and Rahman, A. (2019). Clay mineral compositions in surface sediments of the Ganges-Brahmaputra-Meghna river system of Bengal basin, Bangladesh. *Mar. Geology* 412, 27–36. doi: 10.1016/j.margeo.2019.03.007

Kolla, V., Moore, D. G., and Curry, J. R. (1976). Recent bottom-current activity in the deep western Bay of Bengal. *Mar. Geology* 21, 255–2270. doi: 10.1016/0025-3227(76)90010-4

Kolla, V., and Pierre, E. B. (1973). Clay mineralogy and sedimentation in the eastern Indian ocean. *Deep-Sea Res.* 20, 727–7738. doi: 10.1016/0011-7471(73)90088-0

Li, J. R., Liu, S. F., Shi, X. F., Feng, X. L., Fang, X. S., Cao, P., et al. (2017). Distributions of clay minerals in surface sediments of the middle Bay of Bengal: Source and transport pattern. *Continental Shelf Res.* 145, 59–67. doi: 10.1016/j.csr.2017.06.017

Li, J. R., Liu, S. F., Shi, X. F., Zhang, H., Fang, X., Chen, M., et al. (2018). Clay minerals and Sr-Nd isotopic composition of the Bay of Bengal sediments: Implications for sediment provenance and climate control since 40 ka. *Quaternary Int.* 493, 50–58. doi: 10.1016/J.QUAINT.2018.06.044

Liu, J. H. (2004). The geochemistry of REEs and Nd isotope in deep-sea sediments from the eastern pacific and their geological implications. *Chinese Academy Sci.* 1–137.

Liu, D. B. (2012). Recent progress on studies of the spatial structure and dynamics for the younger dryas event. *Geological Rev.* 58 (02), 341–349. doi: 10.3969/j.issn.0371-5736.2012.02.016

Liu, Z. F., Trentesaux, A., Clemens, S. C., Colin, C., Wang, P. X., Huang, B. Q., et al. (2003). Clay mineral assemblages in the northern south China Sea: implications for East Asian monsoon evolution over the past 2 million years. *Mar. Geology* 201 (1-3), 133–146. doi: 10.1016/S0025-3227(03)00213-5

Liu, Z. J., Yu, J., Sun, X. Y., Zhang, R. R., Sun, S. J., and Zhang, H. (2016a). A discussion of marine sediments ^{14}c data integration and correction. *Quaternary Stud.* 36 (2), 492–502. doi: 10.11928/j.issn.1001-7410.2016.02.24

Liu, Z., Zhao, Y., Colin, C., Stattegger, K., Wiesner, M., Zhang, Y. W., et al. (2016b). Source-to-sink transport processes of fluvial sediments in the south China Sea. *Earth-Science Reviews: Int. Geological J. Bridging Gap between Res. Articles Textbooks* 153, 238–273. doi: 10.1016/j.earscirev.2015.08.005

Lupker, M, France-Lanord, C, and Galy, V. (2013). Increasing chemical weathering in the Himalayan system since the Last Glacial Maximum[J]. *Earth Planetary Sci. Lett.* 365, 242–252. doi: 10.1016/j.epsl.2013.01.038

McLennan, S. M. (1989). Rare earth elements in sedimentary rocks; influence of provenance and sedimentary processes. *Rev. Mineralogy Geochemistry* 21, 169–200. doi: 10.1515/9781501509032-010

Meng, X. W., Du, D. W., Chen, Z. H., and Wang, X. Q. (2000). Factors controlling spatial variation of ^{87}Sr/^{86}Sr in the fine-grained sediments from the overbanks of the yellow river and Yangtze river and its implication for provenance of marine sediments. *Geochimical* 29 (6), 562–569. doi: 10.3321/j.issn:0379-1726.2000.06.008

Milliman, J. D., and Meade, R. H. (1983). World-wide delivery of river sediment to the oceans. *J. Geology.* 91 (1), 1–21. doi: 10.1086/628741. 1983.

Peirce, J. W. (1968). The origin of ninety east ridge and the northward motion of Indian, based on DSDP paleomagnetics [D]. *Boston: MIT Woods Hole Oceanographic Institution*, 40–46.

Phillips, S. C., Johnson, J. E., Underwood, M. B., Guo, J., Giosan, L., and Rose, K. (2014). Long-timescale variation in bulk and clay mineral composition of Indian continental margin sediments in the Bay of Bengal, Arabian Sea, and Andaman Sea. *Mar. Petroleum Geology* 58, 117–138. doi: 10.1016/j.marpetgeo.2014.06.018

Prakash, K. R., and Pant, V. (2019). On the wave-current interaction during the passage of a tropical cyclone in the Bay of Bengal. *Deep Sea Res. Part II* 172, 104658. doi: 10.1016/j.dsr2.2019.104658

Pringle, M. S., Gahagan, L. A., Muller, R. D., Gladczenko, T. P., Duncan, R. A., Coffin, M. F., et al. (2002). Kerguelen hotspot magma output since130 ma. *Petrology* 43 (7), 1121–1139. doi: 10.1093/petrology/43.7.1121

Schott, F. A., and McCreary, J. P. (2001). The monsoon circulation of the Indian ocean. *Prog. Oceanogr* 51 (1), 1–123. doi: 10.1016/S0079-6611(01)00083-0

Scott, R. B., and Xu, Y. (2009). An update on the wind power input to the surface geostrophic flow of the world ocean. *Deep-Sea Res. I* 56, 295–304. doi: 10.1016/j.dsr.2008.09.010

Shankar, D., Vinayachandran, P. N., and Unnikrishnan, A. S. (2002). The monsoon currents in the north Indian ocean. *Prog. Oceanogr* 52 (1), 63–120. doi: 10.1016/S0079-6611(02)00024-1

Shao, L., Qiao, P. J., Pang, X., Wei, G. J., Li, Q. Y., Miao, W. L., et al. (2009). Nd Isotopic variations and its implications in the recent sediments from the northern south China Sea. *Chin. Sci. Bull.* 54 (2), 311–317. doi: 10.1007/s11434-008-0453-8

Song, Z., Wan, S., Colin, C., Yu, Z., Revillon, S., Jin, H., et al. (2021). Paleoenvironmental evolution of south Asia and its link to Himalayan uplift and climatic change since the late Eocene. *Global planetary Change* 200 (May), 103451–103459. doi: 10.1016/j.gloplacha.2021.103459

Stow, D. A. V. (1990). Sediment facies and processes on the Bengal fan, leg 116. *Proc. Ocean Drilling Program Sci. Result* 116, 337–396. doi: 10.2973/odp.proc.sr.116.110.1990

Tang, Y. J., Jia, J. Y., and Xie, X. D. (2002). Environment significance of clay minerals. *Earth Sci. F rontiers* 9 (02), 337–344. doi: 10.3321/j.issn:1005-2321.2002.02.011

Trentesaux, A., Liu, Z., Colin, C., Boulay, S., and Wang, P. (2003). 22. Data Report: Pleistocene Paleoclimatic Cyclicity of Southern China: Clay Mineral Evidence Recorded in the South China Sea (ODP Site 1146). *Red* 15 (20), 25. doi: 10.2973/odp.proc.sr.184.210.2003

Tripathy, G. R., Singh, S. K., Bhushan, R., and Ramaswamy, V. (2011). Sr-Nd Isotope composition of the Bay of Bengal sediments: Impact of climate on erosion in the himalaya. *Geochemical J.* 45 (3), 175–186. doi: 10.2343/GEOCHEMJ.1.0112

Tripathy, G. R., Singh, S. K., and Ramaswamy, V. (2014). Major and trace element geochemistry of Bay of Bengal sediments: Implications to provenances and their controlling factors. *Palaeogeography Palaeoclimatology Palaeoecology: Int. J. Geo-Sciences* 397, 20–30. doi: 10.1016/j.palaeo.2013.04.012

Webber, B. G. M., Matthews, A. J., Vinayachandran, P. N., Neema, C. P., Sanchez-Franks, A., Vijith, V., et al. (2018). The dynamics of the southwest monsoon current in 2016 from high-resolution *in situ* observations and models. *J. Phys. Oceanogr* 48, 2259–2282. doi: 10.1175/JPO-D-17-0215.1

Weber, M. E., Lantzsch, H., Dekens, P., Das, S. K., Reilly, B. T., Martos, Y. M., et al. (2018). 200,000 years of monsoonal history recorded on the lower Bengal fan - strong response to insolation forcing. *Global Planetary Change* 166, 107–119. doi: 10.1016/j.gloplacha.2018.04.003

Weber, M. E., Wiedicke-Hombach, M., Kudrass, H. R., and Erlenkeuser, H. (2003). Bengal Fan sediment transport activity and response to climate forcing inferred from sediment physical properties, sediment. *Or. Geol* 155, 361–381. doi: 10.1016/S0037-0738(02)00187-2

Wei, H. L., Fang, N. Q., Ding, X., Nie, L. S., and Liu, X. M. (2007). Major environmental events reflected by pelagic records since 3.5 ma BP in the ninetyeast ridge at the equator. *Geological Bull. China* 26 (12), 1627–1632. doi: 10.3969/j.issn.1671-2552.2007.12.016

Zhang, Z. G., Fang, N. Q., Li, W. B., Li, J. S., Gui, B. L., and Cui, Y. (2007). The characteristics of the non-$CaCO_3$ grain size of pelagic sediment from the ninety-east ridge and its indicated significance of environment. *J. Taiyuan Univ. Technol.* 38 (1), 85–87. doi: 10.3969/j.issn.1007-9432.2007.01.025

Zhang, Z. F., Fang, N. Q., Wu, L., Wang, J. Q., and Liu, R. M. (2004). Sedimentary records and asian monsoon in ninetyeast ridge of Bay of Bengal since pliocene time. *Earth Sci. - J. China Univ. Geosciences* 29 (2), 157–161.

Zhang, L. L., and Zhou, P (2012). Analysis on the development status of isotope dating technique of marine sediment. *Sci. Technol. Information* 425 (33), 93–112. doi: 10.3969/j.issn.1001-9960.2012.33.063